Micro-patterned photo-aligned ferroelectric liquid crystal Fresnel zone lens

A. K. Srivastava,[1,*] X. Wang,[1,2,4] S. Q. Gong,[2] D. Shen,[2] Y. Q. Lu,[3] V. G. Chigrinov,[1] and H. S. Kwok[1]

[1]State Key Laboratory on Advanced Displays and Optoelectronics Technologies, Hong Kong University of Science and Technology, Hong Kong, China

[2]Physics Department, East China University of Science and Technology, Shanghai 200237, China

[3]National Laboratory of Solid State Microstructures, Collaborative Innovation Center of Advanced Microstructures and College of Engineering and Applied Sciences, Nanjing University, Nanjing 210093, China

[4]e-mail: xqwang@ecust.edu.cn

*Corresponding author: abhishek_srivastava_lu@yahoo.co.in

Received January 26, 2015; revised March 2, 2015; accepted March 12, 2015; posted March 13, 2015 (Doc. ID 233102); published April 3, 2015

In this Letter, we disclose a fast switchable Fresnel zone lens (FZL) by confining the ferroelectric liquid crystals (FLCs) in multiple microscopically defined photo-aligned alignment domains. The photo-alignment (PA) offers good control on the anchoring energy (W) by mean of irradiation doses (ID) and thus excellent alignment for FLCs. Two operational modes of the FLCFZL, i.e., FOCUS/OFF and FOCUS/DEFOCUS, were demonstrated. The proposed diffracting element provides fast response time, high diffraction efficiency (η), with saturated electro-optical (EO) operations up to high frequency (≈2 kHz). Thus, the proposed FLCFZLs with simple fabrication open several opportunities to improve the quality of existing devices and to find new applications.

OCIS codes: (220.0220) Optical design and fabrication; (230.0230) Optical devices; (250.6715) Switching.
http://dx.doi.org/10.1364/OL.40.001643

The liquid crystals (LCs) because of their ability to modulate the light for both phase and amplitude became one of the most promising candidates for versatile optical applications [1–5]. The switchable LCFZL lenses are one of them that has been extensively explored recently and applied for optical information processing, 3D display, optical communication, incision surgeries, and space navigation, etc. [5–15]. The binary-phase FZL focuses the light when the phase difference between two adjacent zones is equal to an odd multiple of π [11]. As compared with conventional LC lenses, LCFZLs is simpler to fabricate with large aperture size. There are two common approaches to fabricate the LCFZL. The first approach deploys patterned electrodes to generate a specific electric field (E) distribution to control the LC director locally. The second approach deals with pre-guided LC directors to realize a specific refractive index distribution that includes patterned polymer-relief, polymer-dispersed LCs, polymer-stabilized LCs, dye-doped LCs, and UV-modified alignment film, etc. [15].

Recently, Lin *et al.* have proposed polarization-independent LCFZL based on surface-mode switching of 90° twisted-nematic LCs by using patterned electrodes [16] where the η is ∼5% OFF-state and ∼25% in the ON-state with switching time (τ) ∼9 ms. Another approach utilized blue phase LCs for the same where $\eta \sim 34\%$ and $\tau \sim 150$ ms [17]. However, a high driving voltage (∼100 V) is needed for fast EO modulations. Alternatively Fan *et al.* have proposed an FZL using polymer-stabilized LCs [6] with $\eta \sim 23\%$ and $\tau \sim 13.5$ ms. However, the diffraction in off-state, because of the index mismatching, is an issue. Recently, we disclosed LCFZL based on the patterned alignment of nematic LC [5].

These approaches show low η, complicated fabrication, higher driving voltage, and larger τ. However, FLCs are known for fast EO response at low E, but there are several issues to be solved [18,19]. Nevertheless, the PA provides an opportunity to translate the advantages of FLCs into a real efficient device. In this Letter, we disclose a method to fabricate a FLCFZL based on patterned PA with two switchable modes (i.e., FOCUS/OFF and FOCUS/DEFOCUS). The PA FLCFZL in both modes shows total $\tau(\tau_{ON} + \tau_{OFF}) < 130$ μs at $E < 7$ V/μm, wherein the PA FLCFZL works under the electrically suppressed helix FLCs (ESHFLCs) mode [20]. The most critical problem of FLCs for photonics is the intrinsic diffraction that appears because of the ferroelectric domains and periodic structure of the FLC helix [21]. However ESHFLCs, due to a special constraint on the FLC helix and W, provide outstanding optical quality with high optical contrast without any intrinsic diffraction lobes [20]. Therefore, it can be exploited for the patterned alignment to generate the desired refractive index distribution and thus various photonic elements, e.g., FZL.

Recently it has been observed that a proper balance between the W and elastic energy (E_k) of the helix for cell gap (d) larger than the FLC pitch provides good alignment for FLCs [20]. In this condition, the helix is not affected by surfaces and provides excellent alignment. However, application of small E [larger than the critical field of helix unwinding (E_c), usually ∼0.1–1 V/μm] compel the helix to unwind and show same dynamics as surface stabilized FLC [20]. Thus, within this constraint, the chosen FLC FD4004N from Dainippon Ink & Chemicals Ltd. Japan (DIC) shows phase transition scheme as $SmC* \rightarrow SmA \rightarrow N* \rightarrow Iso$ at temperatures of 72°C, 85°C, and 105°C, respectively. At room temperature, the FLC helix pitch is (ρ) = 350 nm, spontaneous polarization (P_s) = 61 nC/cm^2, and tilt angle is $\theta = 22.5°$. The E_k of the FLC helix is ∼890 J/m^3 thus

for good alignment W, for $d = 1.5$ μm, should be $\sim 6 \times 10^{-4}$ J/m^2 [22].

Furthermore a sulfonic azo dye SD1 (DIC), because of the wide tunable range of W by means of ID, has been used as a PA layer. The irradiation of polarized light ($\lambda = 450$ nm) results in reorientation of the easy axis (EA) perpendicular to the polarization azimuth of the irradiating light [23]. An important feature of the SD1 is re-writability of the EA, by further exposure, that gives possibility to realize a multi-domain alignment pattern with microscopically defined EA. Furthermore, the W of such PA can be tuned by the ID, which, in the present case, has been fixed at ~ 3 J/cm^2 (for $\lambda = 450$ nm) that provides $W \sim 6 \times 10^{-4}$ J/m^2.

The fabrication of the FZL includes two-step alignment processes. First, the uniform alignment, without any pattern, has been made, on both glass plates of the FLCFZL cell coated with SD1 [24], and the cell was assembled afterward. In the second step, the cell has been irradiated again, through an FZL photo-mask, with a light of polarization azimuth orthogonal to the first step. This approach creates two alignment domains simultaneously on both surfaces (i.e., on top and bottom) without any mutual shifting. Thus, no precise adjustment is required for all patterns, which makes the fabrication relatively simpler. However, ID in both steps should be comparable to provide the similar W in both alignment domains to comply with the requirements of the ESHFLCs [24].

The schematic of the FLC director distribution in the two domains is described in Fig. 1(A). Here δ is the cone angle of the FLC, and β is the angle between the easy axes of the two alignment domains. Under the crossed polarizer, such geometry can be abstracted in Fig. 1(B), where α is the angle between the polarizer and analyzer, while γ is the angle between one of the switching position of either domains and the polarization azimuth of the impinging light. Based on the FLC EO and EA in two adjacent domains [Fig. 1(B)], two switchable modes are possible, i.e., FOCUS/OFF and FOCUS/DEFOCUS.

FOCUS/OFF and FOCUS/DEFOCUS switchable mode FLCFZL share the same configuration except the EA definition in the two adjacent alignment domains. For the FOCUS/OFF mode, where the output light switches between diffractive (FOCUS) and dark (OFF) state on applying E, $\beta = 90°$ [Fig. 1(C)]. However for the FOCUS/DEFOCUS, where the output light is modulated between diffraction (FOCUS) and transmission (DEFOCUS) state, $\beta = 45°$ [Fig. 1(D)]. Furthermore for the FOCUS/OFF mode, the FLCFZL is placed between the crossed polarizers with one of the switching position in the two alignment domain parallel to the polarizer/analyzer. While, for the FOCUS/DEFOCUS mode we need different conditions that has been discussed later in the article.

The normally impinging light on the two domain of the FLCFZL, which has two states as described in Fig. 1(A). The light passing, with polarization azimuth along x axis, through the FLCFZL in state I domain I is $\vec{E}_{\text{in}} = E_0[1\ 0]$. Thus, the output light after the polarizer, the FLC, and the analyzer can be written as

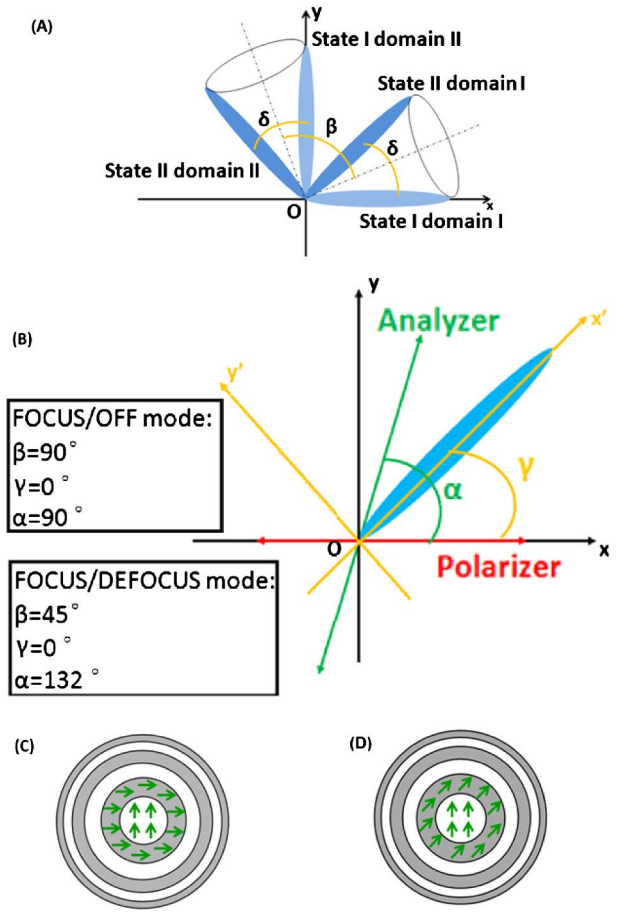

Fig. 1. (A) In state I, the orientation of FLC molecules in domain I and domain II has an angle of β to x axis simultaneously. In state II, the orientation of FLC molecules in each domain rotates an angle of δ simultaneously. (B) Polarizer is along x axis. In the EA of FLCs in state I, domain I has an angle of γ to x axis. Analyzer has an angle of α to x axis. Directors (green arrows) of FLC in Fresnel odd zones (white) and even zones (gray) in (C) and (D). The orientations of EA in two adjacent zones (C) $\beta = 90°$. (D) $\beta = 45°$.

$$\vec{E}_{\text{out}} = \begin{bmatrix} \cos(-\alpha) & \sin(-\alpha) \\ -\sin(-\alpha) & \cos(-\alpha) \end{bmatrix} \begin{bmatrix} 1 & 0 \\ 0 & 0 \end{bmatrix} \begin{bmatrix} \cos\alpha & \sin\alpha \\ -\sin\alpha & \cos\alpha \end{bmatrix} \times \begin{bmatrix} \cos(-\gamma) & \sin(-\gamma) \\ -\sin(-\gamma) & \cos(-\gamma) \end{bmatrix} \begin{bmatrix} 1 & 0 \\ 0 & e^{-i\Gamma_1} \end{bmatrix} \times \begin{bmatrix} \cos\gamma & \sin\gamma \\ -\sin\gamma & \cos\gamma \end{bmatrix} \begin{bmatrix} 1 & 0 \\ 0 & 0 \end{bmatrix} E_0 \begin{bmatrix} 1 \\ 0 \end{bmatrix},$$

where $\Gamma_1 = \frac{2\pi}{\lambda}\Delta n_1 d_1 = \frac{2\pi}{\lambda}\Delta n_1 \frac{\lambda}{2\Delta n_1} = \pi$, and $\vec{E}_{\text{out}} = E_0 \cos(2\gamma - \alpha)\begin{bmatrix}\cos\alpha \\ \sin\alpha\end{bmatrix}$. The E in state i domain j as $E_{i,j}$, where $i = 1, 2$ represent state I and state II, respectively, while $j = 1,\ 2$ represent domain I and domain II, respectively.

Hence the E vector of the light from different domains in different state can be defined as $E_{1,1} = \cos(2\gamma - \alpha)$, $E_{1,2} = \cos(2(\gamma + \beta) - \alpha)$, $E_{2,1} = \cos(2(\gamma + 43°) - \alpha)$, and $E_{2,2} = \cos(2(\gamma + \beta + 43°) - \alpha)$. Thus for maximum η in state I, $E_{1,1}$ and $E_{1,2}$ should have different sign but the same magnitude (~ 1) so that the E in two domains have π phase shift. Whereas for maximum transmittance in

state II, $E_{2,1}$ and $E_{2,2}$ should have same sign and the same magnitude ($\sim$1) so that the E in two domains are in phase. Thus, an optimization function (F) can be defined as follows:

$$F = [(E_{1,1} \cdot E_{1,2} + 1)^2 + (E_{1,1} + E_{1,2})^2] + [(E_{2,1} \cdot E_{2,2} - 1)^2 + (E_{2,1} - E_{2,2})^2]. \quad (1)$$

After scanning β, γ, and α, the F has been minimized to obtain the optimal parameters. The optimal parameters for FOCUS/DEFOCUS mode are $\beta = 45°$, $\gamma = 0°$, and $\alpha = 132°$. In this case, the theoretical limits for η and transmittance are $\sim$18% and 50%, respectively. Whereas for FOCUS/OFF mode, dark state is extremely important, and therefore, the optimized parameter are $\beta = 90°$, $\gamma = 0°$, and $\alpha = 90°$ so $E_{1,1} = E_{1,2} = 0$ and $E_{2,1} = E_{2,2} = 0.998$. In this case, theoretically η in state II is $\sim$40.4%.

The two FLCFZL cells have been designed to meet the equation: $R_k \approx \sqrt{k\lambda f}$, where R_k is the radius of the k_{th} ring, f is the focal distance of the FZL, and d is set to meet the half-wave condition for $\lambda = 632.8$ nm. The microphotographs of the two FLCFZL under crossed polarizers are shown in Fig. 2. Figure 2(A) shows the FLCFZL (radius of the innermost circle $R_{in} = 360$ μm) with $\beta = 90°$, the blue lines indicate the alignment directions. Figures 2(B) and 2(C) show the FLCFZL in two switching positions, in presence of E. Figure 2(D) illustrates another FLCFZL ($R_{in} = 255$ μm) with angle $\beta = 45°$. Figures 2(E) and 2(F) show the two switching states in presence of E.

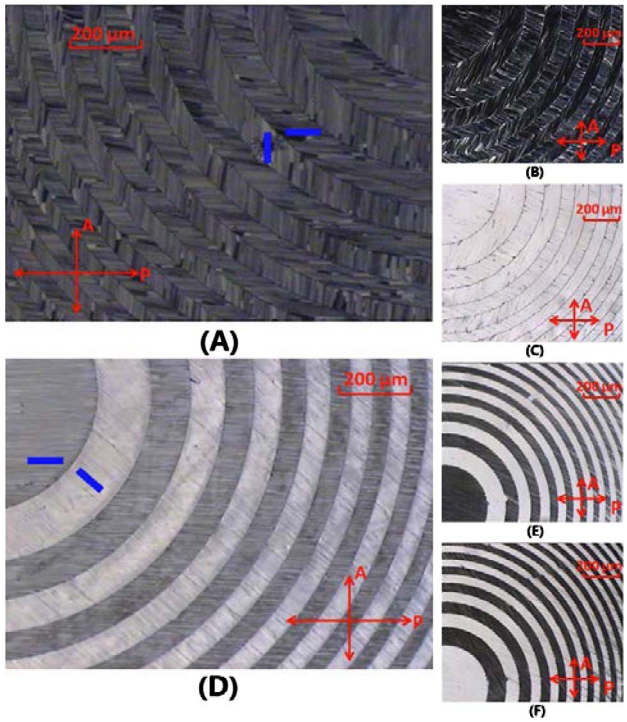

Fig. 2. Microphotographs of two designed FLCFZL under crossed polarizers. The blue lines indicate the alignment directions. (A) FLCFZL ($R_{in} = 360$ μm) with $\beta = 90°$. (B) The same cell as (A) in the state I. (C) The same cell as (A) in the state II. (D) FLCFZL ($R_{in} = 255$ μm) with $\beta = 45°$. (E) The same cell as (D) in the state I. (F) The same cell as (D) in the state II.

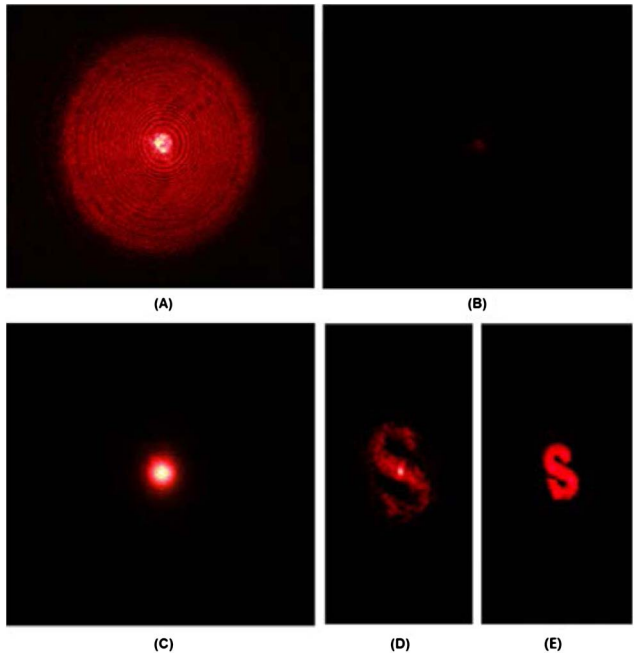

Fig. 3. Diffraction profiles. (A) Diffraction profiles in FOCUS state. (B) Pattern in OFF state of the FOCUS/OFF mode. (C) Represents the pattern in DEFOCUS state for the FOCUS/DEFOCUS mode. (D) Letter "S" in FOCUS state. (E) Letter "S" in DEFOCUS state.

The Figs. 3(A) and 3(B) show diffraction profiles for FOCUS and OFF state of the FOCUS/OFF mode. The η for FOCUS/OFF switchable FLCFZL was measured $\sim$37%, which is close to the theoretical limit. Whereas, the diffraction profile of the DEFOCUS state of the FOCUS/DEFOCUS mode is shown in Fig. 3(C), however the FOCUS state of both modes is the same. The measured η for FOCUS/DEFOCUS switchable FLCFZL is $\sim$14.5%. The transmittance for the DEFOCUS state is $\sim$45.5%, with theoretical limit of 50%. The air-glass reflection, the imperfect polarizers, and some defects in the FLC layers can be attributed for the small discrepancy in theory and experiments. The lens effect of the fabricated FOCUS/DEFOCUS mode FLCFZL is illustrated in Figs. 3(D) and 3(E) in focused and defocused state, respectively, and a mask with transparent letter "S" was placed in between the FLCFZL and the incident light at a distance of 25 cm from the FLCFZL, and the projected image is captured at a distance of 30 cm from the FLCFZL.

Another important key feature of FLCFZL is the EO that is at least 15–20 times faster than other LCFZL. The bottom insertion (a) of Fig. 4 shows the experimental arrangement used to measure different parameters. The η increases at higher voltages from 17% and saturates to 37% after 2 V. The insertion (b) shows the EO response of the proposed FLCFZL that manifest saturated EO modulations up to 2 kHz. This behavior can be explained by the simple EO of the ESHFLCs [20]. The τ decreases at higher voltages at the $E = 6.5$ V/μm and frequency of 1 kHz, the total τ ($\tau_{\text{ON}} + \tau_{\text{OFF}}$) is around 120 μs.

In summary, we disclosed a microscopically patterned PA method to produce ESHFLC-based FLCFZLs, which is characterized by two modes, i.e., FOCUS/OFF

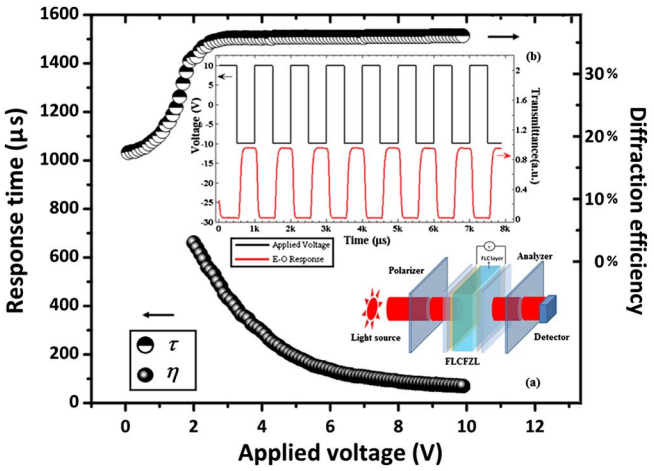

Fig. 4. Shows voltage dependence of τ and voltage dependence of η. The insertion (a) shows experimental arrangement where FLCFZL cell is placed in between two polarizers. The insertion (b) shows EO response of the FLCFZL cell, top is the applied voltage, and in bottom represents EO response at temperature $\lambda = 0.63$ μm and frequency 1 kHz.

and FOCUS/DEFOCUS modes depending on β. The FLCFZL combines good optical quality with very fast EO response at very low driving voltage without intrinsic diffraction lobes of the FLCs. However, polarization dependence and precise control on the FLC, the PA, and ID in the two-step PA process, makes this technology a bit difficult, and further research is required to make it more tolerant for ID. However, the proposed FLCFZLs with extreme EO have vast potential for application in modern devices.

This work is supported by Partner State Key Laboratory on Advanced Displays and Optoelectronics Technologies HKUST, and the National Natural Science Foundation of China (61490714 and 61435008).

References

1. X. Ren, S. Liu, and X. Zhang, Proc. SPIE **5456**, 391 (2004).
2. T. Grulois, G. Druart, N. Guérineau, A. Crastes, H. Sauer, and P. Chavel, Opt. Lett. **39**, 3169 (2014).
3. P. Valley, D. L. Mathine, M. R. Dodge, J. Schwiegerling, G. Peyman, and N. Peyghambarian, Opt. Lett. **35**, 336 (2010).
4. M. Hain, W. Spiegle, M. Schmiedchen, T. Tschudi, and B. Javidi, Opt. Express **13**, 315 (2005).
5. C. H. Lin, Y. Y. Wang, and C. W. Hsieh, Opt. Lett. **36**, 502 (2011).
6. Y. H. Fan, H. W. Ren, and S. T. Wu, Opt. Express **11**, 3080 (2003).
7. S. C. Jeng, S. J. Hwang, J. S. Horng, and K. R. Lin, Opt. Express **18**, 26325 (2010).
8. E. Buckley, Opt. Lett. **35**, 3399 (2010).
9. D. W. Kim, C. J. Yu, H. R. Kim, S. J. Kim, and S. D. Lee, Appl. Phys. Lett. **88**, 203505 (2006).
10. C. J. Hsu, C. H. Liao, B. L. Chen, S. Y. Chih, and C. Y. Huang, Opt. Express **22**, 25925 (2014).
11. H. Ren, Y. H. Fan, and S. T. Wu, Appl. Phys. Lett. **83**, 1515 (2003).
12. L. C. Lin, H. C. Jau, T. H. Lin, and A. Y. Fuh, Opt. Express **15**, 2900 (2007).
13. W. C. Hung, Y. J. Chen, C. H. Lin, I. M. Jiang, and T. F. Hsu, Appl. Opt. **48**, 2094 (2009).
14. K. C. Lo, J. D. Wang, C. R. Lee, and T. S. Mo, Appl. Phys. Lett. **91**, 181104 (2007).
15. X. Q. Wang, A. K. Srivastava, V. G. Chigrinov, and H. S. Kwok, Opt. Lett. **38**, 1775 (2013).
16. X. Q. Wang, F. Fan, T. Du, A. M. W. Tam, Y. Ma, A. K. Srivastava, V. G. Chigrinov, and H. S. Kwok, Appl. Opt. **53**, 2026 (2014).
17. C. H. Lin, H. Y. Huang, and J. Y. Wang, IEEE Photon. Technol. Lett. **22**, 137 (2010).
18. V. G. Chigrinov and A. K. Srivastava, Mol. Cryst. Liq. Cryst. **595**, 39 (2014).
19. Y. M. Lou, Q. K. Liu, H. Wang, Y. C. Shi, and S. L. He, Appl. Opt. **49**, 4995 (2010).
20. A. K. Srivastava, W. Hu, V. G. Chigrinov, A. D. Kiselev, and Y. Q. Lu, Appl. Phys. Lett. **101**, 031112 (2012).
21. A. K. Srivastava, J. L. Tocnaye, and L. Dupont, J. Display Technol. **6**, 522 (2010).
22. A. K. Srivastava, E. P. Pozhidaev, V. G. Chigrinov, and R. Manohar, Appl. Phys. Lett. **99**, 201106 (2011).
23. Q. Guo, A. K. Srivastava, E. P. Pozhidaev, V. G. Chigrinov, and H. S. Kwok, Appl. Phys. Express **7**, 021701 (2014).
24. E. A. Shteyner, A. K. Srivastava, V. G. Chigrinov, H. S. Kwok, and A. D. Afanasyev, Soft Matter **9**, 5160 (2013).